

# COMPRESSIVE PROPERTIES OF APPLE CULTIVAR GOLDEN DELICIOUS

Kubik Lubomir

Slovak University of Agriculture in Nitra, Tr. A. Hlinku 2, 949 76 Nitra, Slovak Republic, Lubomir.Kubik@uniag.sk

**Abstract:** The study dealt with the experimental and numerical evaluation of the apple cultivar Golden Delicious (*Malus domestica* L.) at compressive loading in lateral direction. Mechanical properties such as failure stress and strain as well as modulus of elasticity can be used to evaluate the behaviour of the fruits mechanically under the static loading. A testing machine Andlog Stentor 1000 (Andlog Technologies, Vitrolles, France) was employed for compression tests. The behaviour of the hemisphere of fruit was studied between two parallel plates and with the cylindrical indenter of diameter of 8 mm with flat end. The samples of the apples have been tested at the different strain rates. The experiments were performed at twelve velocities from 10 to 350 mm.min<sup>-1</sup> in order to achieve the different strain rates. Compression test of the fruits at the different strain rates corresponds to the quasi – state loading. The influence of strain rate on the stress was studied. The material exhibits nonlinear viscoelastic behaviour. Apparent moduli of elasticity were determined on the base of Hertz theory (ASAE, 2004). The rupture points of the material were determined.

**Key words:** apple, compression, strain rate, rupture point

The instrumental firmness of apples changes significantly during shelf life, whereas the sensory attributes do not change significantly for each cultivar or for each attribute. It confirms advantage of the instrumental firmness measurements compared to the sensory evaluation (Zdunek, 2010). Compression test of the fruits at the different strain rates corresponds to the quasi – state loading (Severa, 2008). The influence of strain rate on the stress was studied. If the material exhibits viscoelastic behavior a Maxwell model with increasing modulus of elasticity can be considered as a simple so called explanatory model, which can explain the stress-strain curves (Csima et al., 2014). The texture of apple flesh is important in assessing the eating qualities of the fruit (Khan and Vicent, 1993). Flesh firmness is a key quality parameter, since it is directly related to fruit ripeness, and is often a good indicator of shelf – life potential (De Keteleere et al., 2006). Vozary and Meszaros (2007) interested in Idared apple cylinder of 20 mm diameter and of 15 mm length, cut out from whole apple in radial direction. The real part of impedance decreased as the deformation, or the stress increased, and the imaginary part of impedance increased under increasing stress or deformation. Extensive test have shown that if the initial part of force-deformation curves of soft biological tissues are taken into consideration, the initial part of the curves are usually concaved towards the force axis. This is exactly opposite the

## MATERIAL AND METHODS

### Samples

The apple fruits of cultivar Golden Delicious (*Malus domestica* L.) were tested. The fruits were obtained in the conventional shop and stored one day at the temperature 4°C and the air humidity (40 – 60) % in the refrigerator. Six fruits were collected and used for the testing. Each fruit was cut into two hemispheres. Twelve samples were used for each sort of the loading. Eleven samples were suitable for elaboration.

### Compression methods

Two type of the loading were realized: the compression of the hemisphere between two parallel plates and the penetration of the hemisphere with the flat – ended indenter with diameter of 8 mm. Statical compressive loading in lateral direction was used for the fruit testing. A testing machine Andlog Stentor 1000 (Andlog Technologies, Vitrolles, France) was applied for compression tests. The experiments were performed at twelve velocities from 10 to 350 mm.min<sup>-1</sup> in order to achieve the different strain rates (Severa, 2008). The force F (N) and the compression D<sub>c</sub> (m) were measured by the acquisition software RSCV ver. 4.06. The loading curves of dependency of the force on the deformation or of the stress on the strain were realized. Compression test of the fruits at the different strain rates corresponds to the quasi – state loading. The influence of the loading speed on the force and the influence of strain rate on the stress were studied. The material exhibited nonlinear viscoelastic behavior. Apparent moduli of elasticity of the apple hemispheres compressed between two parallel plates were determined on the base of the Hertz theory from the equation (ASAE, 2004):

$$E_a = \frac{0.338 K^{\frac{2}{3}} F (1 - \mu^2)}{D_c^{\frac{2}{3}} \left[ \left( \frac{1}{R_c} + \frac{1}{R_c} \right)^{\frac{1}{2}} \right]} \quad (1)$$

where: E<sub>a</sub> is the apparent modulus of elasticity, Pa,

D<sub>c</sub> is the compression, m,

μ represents Poisson's ratio, - ,

F is the force, N,

R<sub>U</sub>, R<sub>D</sub> are the minimum and the maximum radii of curvature of

the convex surface of the sample at the point of contact with the upper plate, m,

K is the constant determined on the base of contact angle.

The method based on the penetration of the fruit hemisphere by flat – ended cylindrical indenter of diameter 8 mm enabled the determination of the apparent moduli of elasticity from the equation (ASAE, 2004):

$$E_a = \frac{0.338 K^{\frac{2}{3}} F (1 - \mu^2)}{D_c^{\frac{2}{3}} \left[ \left( \frac{1}{R_c} + \frac{1}{R_c + d} \right)^{\frac{1}{2}} \right]} \quad (2)$$

where: all quantities are the same as in the equation (1),  
d is the indenter diameter curvature, m.



Figure 1 Compression of the hemisphere between two parallel plates

## RESULTS AND DISCUSSION

The procedure of the compression of fruit hemisphere between two parallel plates is presented in Fig. 1. The parameters of the samples, loading speeds and strain rates are outlined in Table 1. The dependence force – deformation is shown in Fig. 2. The influence of the loading rate on the force during compression was very small and irregular. The data have been converted into stress – strain dependences and are presented in the Fig. 3. The influence of the strain rate on the stress is shown in the Figs. 4, 5 and 6. The dependences were calculated for the strains of 0.1, 0.2 and 0.3 respectively. The material exhibits a typical nonlinear viscoelastic behavior.

**Table 1** Parameters of the hemisphere samples. n – number of sample, R<sub>U</sub>, R<sub>D</sub> – minimum and the maximum radii of curvature of the surface of the sample, S – elliptical area of the sample section, v – loading speed

n	R <sub>U</sub> (mm)	R <sub>D</sub> (mm)	S (mm <sup>2</sup> )	v (mm.min <sup>-1</sup> )	v (mm.s <sup>-1</sup> )	Strain rate (s <sup>-1</sup> )
1	33.48	35.60	3741.97	10	0.1667	0.0047
2	30.78	29.20	2821.70	20	0.3333	0.0114
3	33.25	35.35	3690.72	30	0.5000	0.0141
4	30.90	33.80	3279.48	50	0.8333	0.0247
5	31.53	32.60	3227.03	80	1.3333	0.0409
6	28.03	31.90	2807.15	100	1.6667	0.0522
7	28.85	32.15	2912.44	150	2.5000	0.0778
8	33.65	30.50	3222.66	200	3.3333	0.1093
9	33.15	31.90	3320.50	250	4.1667	0.1306
10	31.93	31.80	3187.78	300	5.0000	0.1572
11	34.60	36.90	4008.96	350	5.8333	0.1581

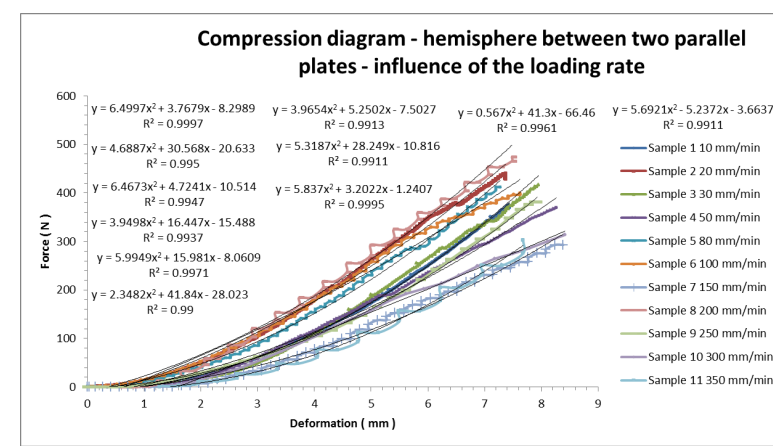


Figure 2 The influence of the loading speed on the force during the hemisphere compression between two parallel plates

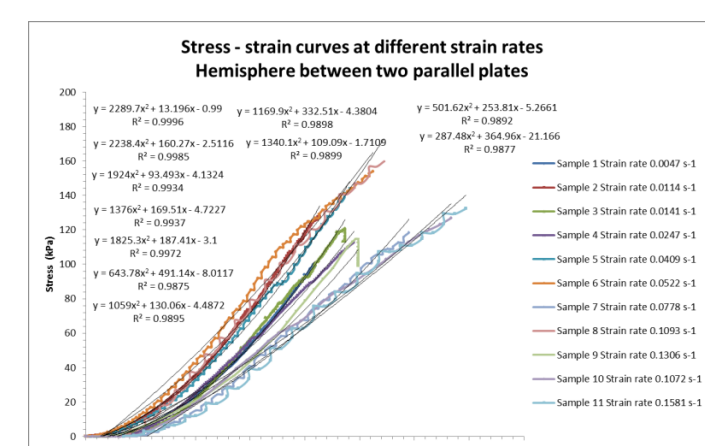


Figure 3 The stress – strain dependences during the compression of the hemispheres between two parallel plates at different strain rates

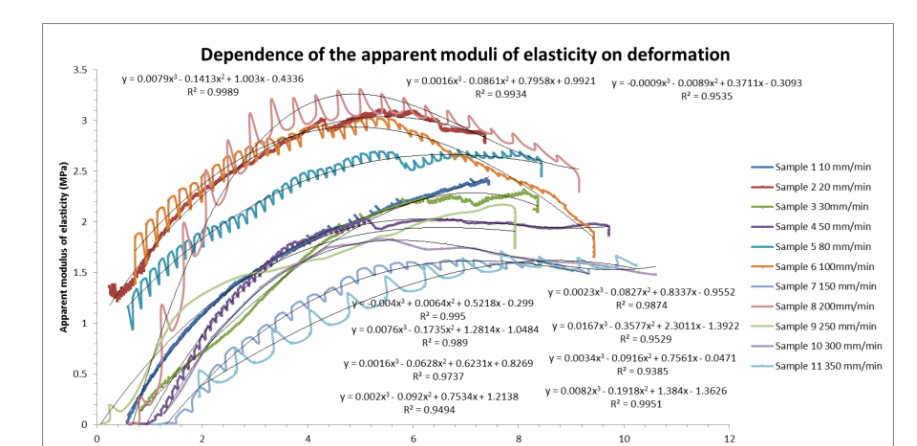


Figure 7 Dependences of the moduli of elasticity on the deformation. Compression between two parallel plates

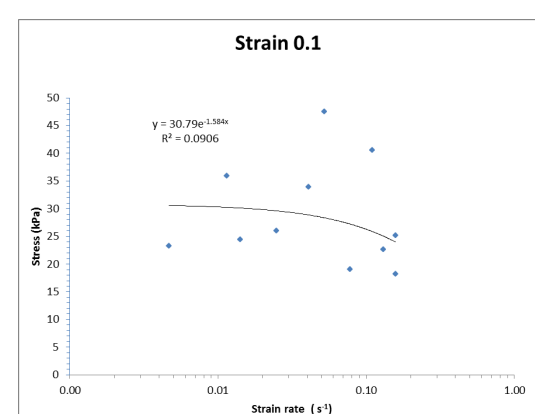


Figure 4 Strain rate influence on the stress at the strain 0.1. Compression between two parallel plates

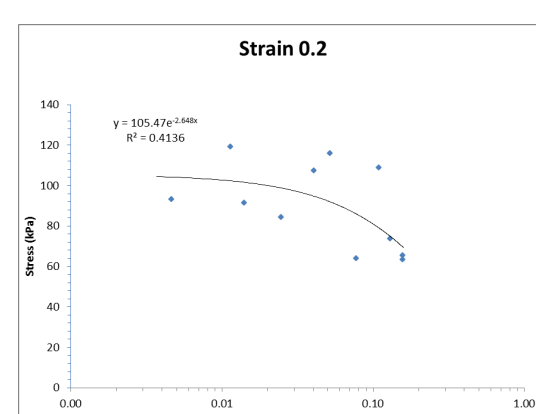


Figure 5 Strain rate influence on the stress at the strain 0.2. Compression between two parallel plates

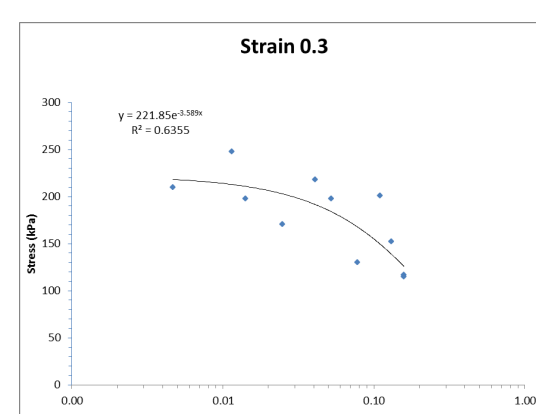


Figure 6 Strain rate influence on the stress at the strain 0.3. Compression between two parallel plates

The regression equations in the Figs. 4, 5 and 6 were applied for the determination of the stresses at the strains 0.1, 0.2 and 0.3 and for the determination of the deformation times of the material at these strains.

**Table 2** Regression coefficients a and b, deformation time t and the stress σ<sub>0</sub> determined from the equations in the Figs. 4, 5, and 6.

Strain	a	b	t (s)	σ <sub>0</sub> (kPa)
0,1	30,79	-1,584	0,462186	30,79
0,2	105,47	-2,648	0,568432	105,47
0,3	221,85	-3,989	0,739443	221,85

Apparent moduli of elasticity were determined from the Eq. 1. Poisson's ratio μ was assumed 0.22 (ASAE, 2004). K was the constant determined on the base of contact angle, K = 1.349. Apparent moduli of elasticity depended on value of the deformation D<sub>c</sub> (mm). Dependences are presented in the Fig. 7. In the level of deformation from 1 mm to 9 mm, realized by the compression between two parallel plates, the experimental values of the apparent moduli of elasticity ranged from 500 kPa to the 3000 kPa.

The penetration of the hemisphere by the flat – ended cylinder indenter of the diameter 8 mm is shown in the Fig. 8. The influence of the loading speed on the force during penetration of the hemisphere by the flat – ended cylinder indenter of the diameter 8 mm is presented in the Fig. 9. The influence of the loading rate on the force during compression was also very small and irregular just at the plate compression. The data have been converted into stress – strain dependences and are presented in the Fig. 10. The influence of the strain rate on the stress is shown in the Figs. 11, 12 and 13. The dependences were calculated for the strains of 0.03, 0.06 and 0.1 respectively. The material also exhibits a typical nonlinear viscoelastic behavior. Rupture points of the mesocarp and the apple's skin were determined from the maximums of the curves in the Figs. 9 and 10. The values of the rupture points of the apple's skin and the mesocarp at the different strain rates are presented in Tab. 3.

**Table 3** Rupture points at the different strain rates. F<sub>R</sub> – rupture force, D<sub>R</sub> – rupture deformation, s<sub>R</sub> – rupture stress, e<sub>R</sub> – rupture strain, n – number of sample

n	Strain rate (s <sup>-1</sup> )	F <sub>R</sub> (N)	D <sub>R</sub> (mm)	σ <sub>R</sub> (kPa)	e <sub>R</sub> (-)
1	0.0047	51.52	3.99	14.04	0.117
2	0.0114	49.92	3.60	17.76	0.124
3	0.0141	58.48	4.97	15.83	0.140
4	0.0247	54.89	4.55	16.74	0.135
5	0.0409	53.47	4.67	16.57	0.143
6	0.0522	39.40	3.72	14.07	0.120
7	0.0778	38.90	4.14	13.36	0.134
8	0.1093	56.53	4.23	17.54	0.139
9	0.1306	60.49	4.83	18.22	0.151
10	0.1572	40.95	3.96	12.85	0.156
11	0.1581	41.40	3.82	10.33	0.104
Average		49.631	4.316	15.210	0.133
Standard dev.		2.436	0.152	0.745	0.005
Variation coeff.		4.908	3.525	4.898	3.556

Figure 8 Penetration of the hemisphere by the flat – ended cylinder indenter

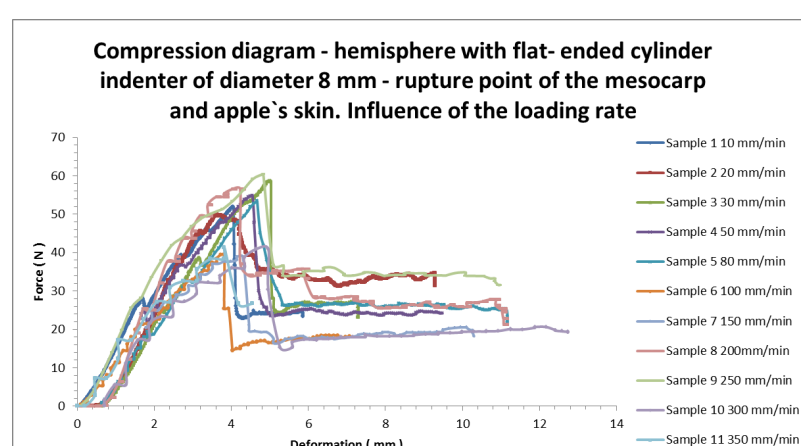


Figure 9 The influence of the loading speed on the force during penetration of the hemisphere by the flat – ended cylinder indenter of the diameter 8 mm. Rupture points of the mesocarp and the apple's skin

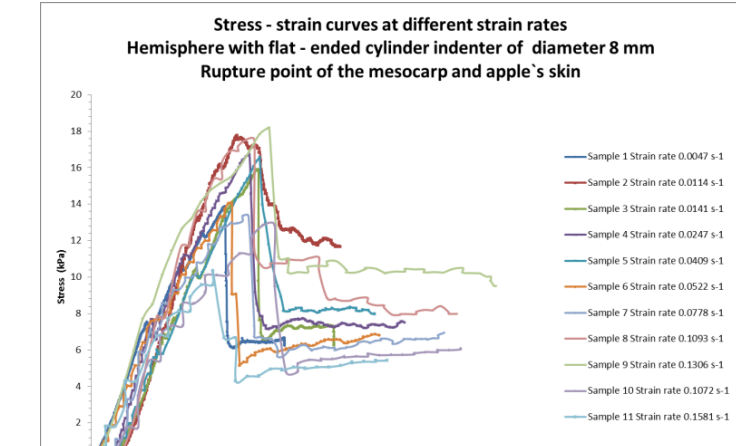


Figure 10 The stress – strain dependences during the penetration of the hemispheres by the flat – ended cylinder indenter at the different strain rates

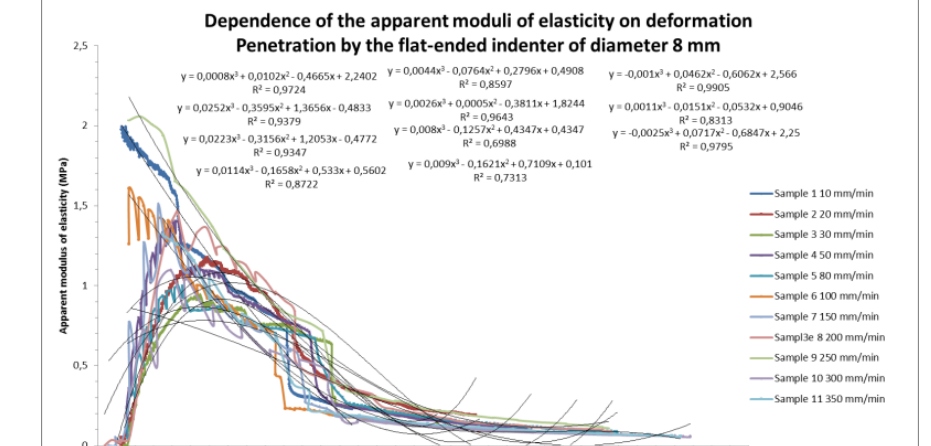


Figure 14 Dependences of the moduli of elasticity on the deformation. Penetration by the flat – ended cylinder indenter

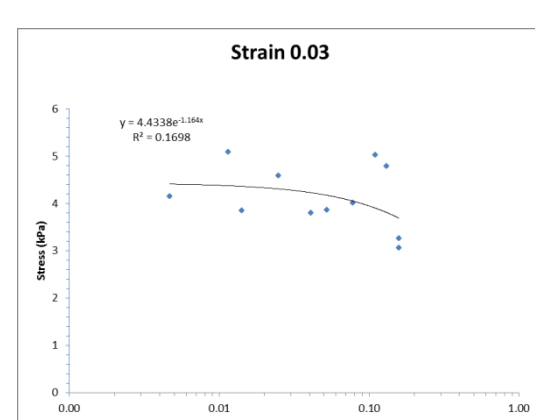


Figure 11 Strain rate influence on the stress at the strain 0.03. Penetration by the flat – ended cylinder indenter of diameter 8 mm

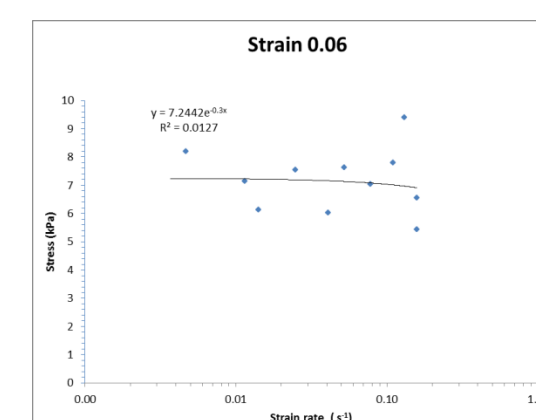


Figure 12 Strain rate influence on the stress at the strain 0.06. Penetration by the flat – ended cylinder indenter of diameter 8 mm

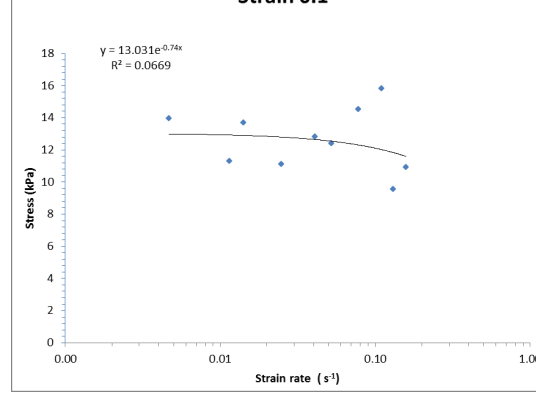


Figure 13 Strain rate influence on the stress at the strain 0.1. Penetration by the flat – ended cylinder indenter of diameter 8 mm

The regression equations in the Figs. 11, 12 and 13 were applied for the determination of the stresses at the strains 0.03, 0.06 and 0.1 and for the determination of the deformation times of the material at these strains.

**Table 4** Regression coefficients a and b, deformation time t and the stress σ<sub>0</sub> determined from the equations in the Figs. 11, 12, and 13.

Strain	a	b	t (s)	σ <sub>0</sub> (kPa)
0,03	4,433	-1,584	1,063747	4,433
0,06	7,244	-2,648	1,337257	7,244
0,10	13,031	-3,989	1,553754	13,031

Apparent moduli of elasticity were determined from the Eq. 2. Poisson's ratio μ was assumed 0.22 (ASAE, 2004). K was the constant determined on the base of contact angle, K = 1.349. Apparent modulus of elasticity depended also on value of the deformation D<sub>c</sub> (mm). Dependences are presented in the Fig. 14. In the level of deformation from 1 mm to 5 mm the experimental values of the apparent moduli of elasticity obtained by the flat – faced cylindrical indenter of diameter 8 mm, ranged from 500 kPa to the 2000 kPa.

## CONCLUSIONS

The measurements did not confirm the influence of the loading rate on the compress force and the influence of the strain rate on the compress stress during the compression of the fruit hemispheres between two parallel plates or during the penetration of the flat – ended indenter of the diameter 8 mm. Great variation of the values was caused by the different dimension of the fruit hemispheres samples, mainly of the diameters and the cross sections of the hemispheres. The dependences of the stress on the strain rate showed low level of the regression, but we could establish the deformation times and the stresses on the level of the constant strain. The apparent moduli of elasticity obtained on the base of Hertz's theory for the lateral loading of the hemispheres between two parallel plates were consistent with the moduli determined by the cylinder flat – ended indenter. The values of the apparent moduli of elasticity depended on the deformation at which were calculated.

## ACKNOWLEDGMENT

The research leading to these results has received funding from the European Community under project no 26220220180: Building Research Centre „AgroBioTech“. Author express the appreciations of the SGA of the ME SR of Slovak Republic and the SAC within the framework of the research were realized in the project Physical properties of biomaterials and the application of physical methods at the evaluation of the specific quality indicators of agricultural materials, No. 1/085400/14.

## REFERENCES

- Alamar, M. C., Vanstreels, E., Oey, M. L., Moltó, E. & Nicolai, B. M. 2008. Micromechanical behaviour of apple tissue in tensile and compression tests: Storage conditions and cultivar effect. *Journal of Food Engineering*, 86:324–333.
- ASAE 2004. Standard S368.4: Compression Test of Food Materials of Convex Shape. American Society of Agricultural Engineering, 2950, Niles Road, ST. Joseph, MI, USA.
- Costa, F., Cappellin, L., Fontanari, M., Longhi, S., Guerra, W., Magnago, P., Gasperi, F. & Biasioli, F. 2012. Texture dynamics during postharvest cold storage ripening in apple (*Malus domestica* Borkh). *Postharvest Biol. Technol.* 69: 54–63.
- Csima Gy., Dénes L., Vozáry E. 2014. A possible rheological model of gum candies. *Acta Alimentaria*, 43, 36 – 44.
- De Keteleere, B., Howarth, M. S., Crezee, L., Lammertyn, J., Viaene, K., Bulens, I. & De Baerdemaeker, J. 2006. Postharvest firmness changes as measured by acoustic and low-mass impact devices: a comparison of techniques. *Postharvest Biol. Technol.* 41: 275–284.
- Khan, A. A. & Vincent, V. F. 1993. Anisotropy in the fracture properties of apple flesh as investigated by crack-opening tests. *Journal of Material Sciences*, 28: 45 – 51.
- Mohsenin, N. N. 1986. *Physical properties of plant and animal materials*. New York: Gordon and Breach Science Publishers, 841 p.
- Severa L. 2008. Behaviour of the peach under underwater shock wave loading. *Acta universitatis agriculturae et silviculturae mendelianae brunensis*, 17, 151–159.
- Shirvani, M., Ghanbarian, D. & Ghasemi – Varnamkhasti, M. 2014. Measurement and evaluation of the apparent modulus of elasticity of apple based on Hooke's, Hertz's and Boussinesq's theories. *Measurement*, 54: 133–139.
- Vozary, E. & Meszaros, P. 2007. Effect of mechanical stress on apple impedance parameters. 13th international conference on electrical bioimpedance and the 8th conference on electrical impedance tomography IFMBE Proceedings. Aug. 29 – Sep 02, 2007, Graz, Austria, 17: 118 – 121.
- Winisdorffer, G., Musse, M., Quellec, S., Barbacci, A., Le Gall, S., Mariette, F. & Lahaye, M. 2015. Analysis of the dynamic mechanical properties of apple tissue and relationships with the intracellular water status, gas distribution, histological properties and chemical composition. *Post-harvest Biology and Technology*, 104: 1–16.
- Zdunek A., Cybulska J., Konopacka D., Rutkowski K. 2011. Inter-laboratory analysis of firmness and sensory texture of stored apples. *Int. Agrophys.* 25, 67 – 75.